Available online www.jsaer.com

***Journal of Scientific and Engineering Research*, 2017, 4(7):169-177**

Review Article

ISSN: 2394-2630
CODEN(USA): JSERBR

Activated Flux TIG Welding of Austenitic Stainless Steels

Memduh Kurtulmuş[1], Mustafa Kemal Bilici[1], Zarif Çatalgöl[2], İrfan Çalış[1]

[1]Marmara University, Applied Science High School,Göztepe Campus, İstanbul
[2]Marmara University Technology Faculty, Goztepe Campus, Istanbul

Abstract The TIG welding with active flux (A-TIG welding) consists in depositing a thin layer of flux on the work piece surface just before the welding. The layer deposition can be done by brushing or spraying over the surface, and welding is performed after it dries out. It is found that with this process it is possible to increase the weld penetration and productivity up to three times higher or more compared to the TIG process in metals. In this review paper, A-TIG welding of austenitic stainless steels is examined. The welding flux, the shielding gas and the welding parameters affect the weld penetration in A-TIG welds. The effects of the activated flux welding mechanisms, the flux chemical composition, thickness of the flux, flux powder size welding current, the arc voltage, the arc length, the welding speed and composition of the shielding gas on weld geometry of austenitic stainless steel A-TIG welds are explained in detail.

Keywords A-TIG welding, austenitic stainless steels, oxide flux, weld penetration

Introduction

Tungsten inert gas (TIG) welding process is known for its versatility and high joint quality. However, these advantages of TIG welding are offset by the limited thickness of material that can be welded in a single pass and by the poor productivity of the process [1]. A new TIG process variant, known as activated flux welding (A-TIG), uses an activating flux to overcome these limitations by increasing the penetration significantly that can be achieved at a given current [2]. The A-TIG welding process in which a very thin coating of the flux is deposited on the joint area prior welding. The flux consists mainly of oxides and halides in the form of thin powder dispersed in an organic solvent, usually acetone. Before starting the A-TIG welding process some time is needed to evaporate the liquid of the paste. The liquid of the paste evaporates within seconds leaving a layer of flux on the surface. Fig. 1 shows the cross-sections of the weld beads obtained during autogenous TIG welding and A-TIG welding of AISI 316L stainless steel, respectively using the same welding process parameters [3]. Deeper weld beads were obtained with the A-TIG welding.

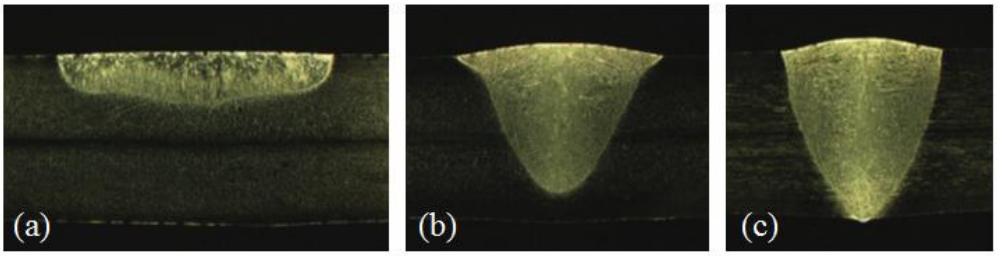

Figure 1: Macrostructure of (a) TIG, (b) TiO_2 flux A-TIG and (c) SiO_2 flux A-TIG welds produced with the same welding parameters on AISI 316L steel plates [3].

Activating Flux Welding Mechanisms

Although, there are several mechanisms were proposed by the researchers, there is not a general agreement about the mechanism of the A-TIG welding process. The proposed theories are the arc constriction, reversal of the Marangoni convection, the arc pressure and Lorentz forces [4]. Among these theories the first two are very important [5,6]. The important theories are explained below. Fig. 2 schematically illustrates the important mechanisms underlying the increased penetration capability of TIG weld produced with an activated flux [7].

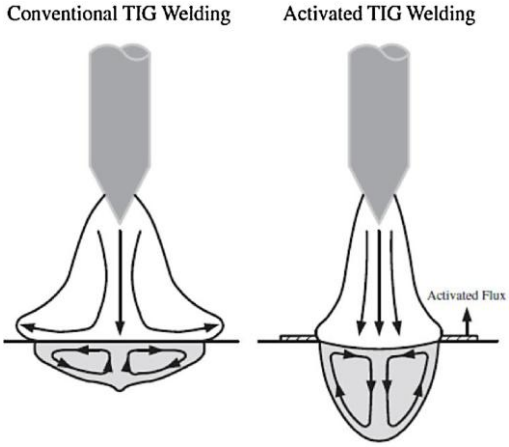

Figure 2: Mechanism for increased penetration capability of activated TIG weld [7].

Arc constriction mechanism: Fig. 3 illustrates the arc columns and the anode roots of TIG and A-TIG welds [3]. Fig. 3 shows that fluxes constrict the arc column and the anode root diameter compared to the conventional TIG arc at the same current level. Each flux has its own characteristic effect. Constriction of the plasma column increases the weld penetration as shown in Fig. 1.

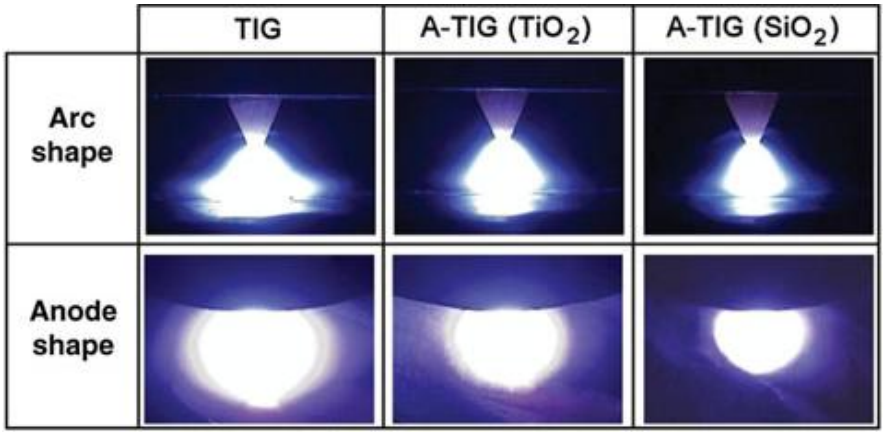

Figure 3: Effect of TIG welding without and with flux on arc column and anode spot of AISI 316L stainless steel plates [3].

In the A-TIG process, it is proposed [8] that arc constriction is produced by the effect of the vaporized molecules capturing electrons in the outer regions of the arc which results in a constricted plasma (Fig. 4). The flux atoms are ionized to generate electrons and positive ions. The reactions occurring primarily in the arc column lead to a reduction in the diameter of the plasma column and, hence, the area of the anode root as shown in Fig. 3. The degree of constriction will be determined by the effectiveness of the flux vapor to combine with the electron [8].

Marangoni convection: The geometry of the weld pool is directly affected with the liquid metal movement [9]: The lateral metal movement forms a wide, shallow weld and the vertical liquid movement produces a deep and

narrow weld pool as shown in Fig. 2. It is well established that surface tension is usually the dominant driving force [1] in TIG welding.

The Marangoni convection refers to the convection movements due to the surface tension gradient on the weld pool surface, as shown in Fig. 5 [9]. While using TIG welding processes, the surface tension gradient is generally negative, and the convection movements are centrifugal [9]. The addition of an activating flux involves an inversion of the convection currents due to the presence of oxygen at the melting zone surface [10]. It originates from dissociation of the oxides in the activating flux [11] and increases the active surface tension [12]. In this case, the surface tension gradient becomes positive, and the resulting convection movements are vertical. Thus, the A-TIG process leads to an increase in penetration depth and a decrease in weld pool width.

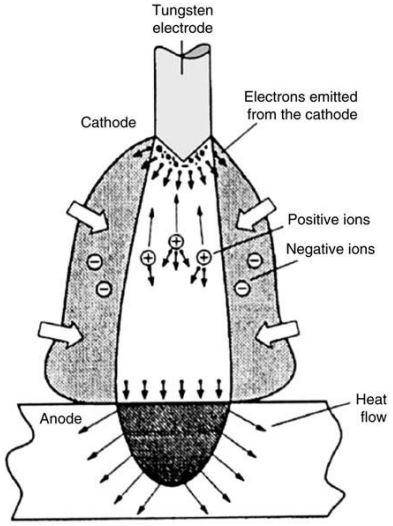

Figure 4: Schematic illustration of model of arc constriction by the activating flux [8].

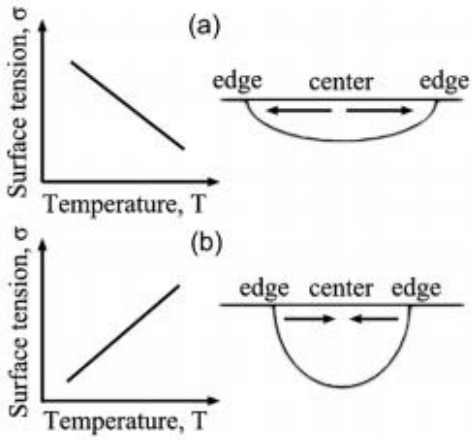

Figure 5: Marangoni convection mode in the weld pool (9): (a) $\partial\sigma/\partial T < 0$; (b) $\partial\sigma/\partial T > 0$.

A-TIG Fluxes

The nature and exact composition of the flux depends on the material to be welded. Several mixtures were published. A patented activating flux formulation for TIG welding of austenitic stainless steel was published: 30-50%TiO_2, 25-40% SiO_2, 10-20% Cr_2O_3, 5-15% NiO and 5-15% CuO [13]. Table 1 illustrates the mono fluxes which were successfully applied in A-TIG welding. Each flux powder has its own characteristic effect in A-TIG welding process. Figure 6 shows the characteristics of the Type 316L stainless steel TIG weld geometry produced with and without flux [13]. Each powder has a characteristic effect.

If the activated flux of the A-TIG welding process consists two or more different powders, the ratio of the mixture becomes important [22]. Figure 7 shows the characteristics of austenitic stainless steel TIG weld

geometry produced with various flux compositions. The increases in weld penetration and the decrease in bead width are significant with use of the activating flux, which is composed of MnO_2 and/or ZnO powder mixture. The 40%MnO_2-60%ZnO mixture led to the greatest improvement in penetration capability.

Table 1: Activating fluxes which gave successful results in A-TIG welding of stainless steels

STAINLESS STEEL TYPE	ACTIVATING FLUXES
Ferritic stainless	TiO_2 [14], B_2O_3 [14], SiO_2 [14]
Austenitic stainless	TiO_2 [15], SiO_2 [15], Cr_2O_3 [15], ZnO[15], Fe_2O_3 [15], MnO_2[15], MoO_3 [15], FeO[16], ZrO_2 [17], CrO_3 [18], AlF_3[19],
Duplex stainless	SiO_2 [20], MoO_3[20], Cr_2O_3[20], TiO_2 [15]
Martensitic stainless	CuO[21], Co_3O_4[21]

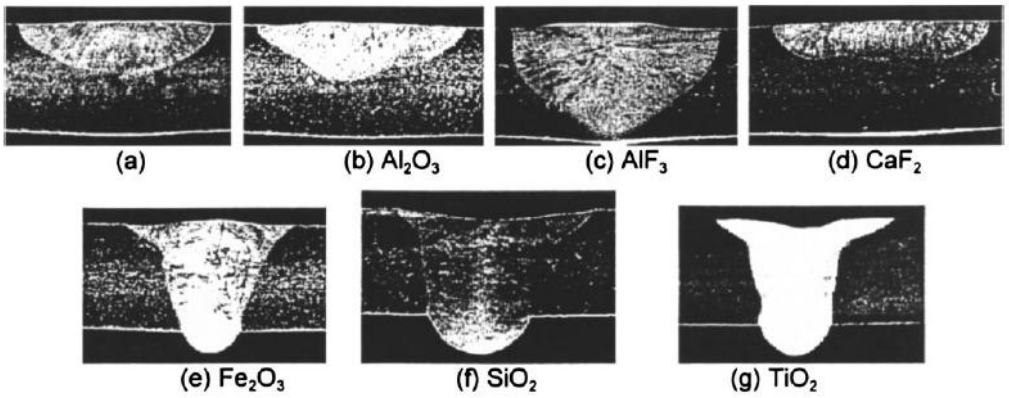

Figure 6: Characteristics of weld geometry produced with and without activated flux [19], (a) TIG welding, (b-g) A-TIG welding

In a study the particle size effect on the weld penetration were investigated to in A-TIG welding of austenitic stainless steels [23]. SiO_2 was used in the experiments. Three kinds of particle sizes were selected to investigate the effect of particle size and the flux quantity on the weld penetration. It is clear that the small particles (0.8 and 4 μm) have a good effect on enhancing the penetration, while the large particle (25 μm) has no effect. The specific surface area of small flux particles are larger than big particles. Since the decomposition of the oxide depends on the reaction rate, which increases with the specific area, the small particle is easily decomposed. This implies that the decomposition of large SiO_2 particles is very weak.

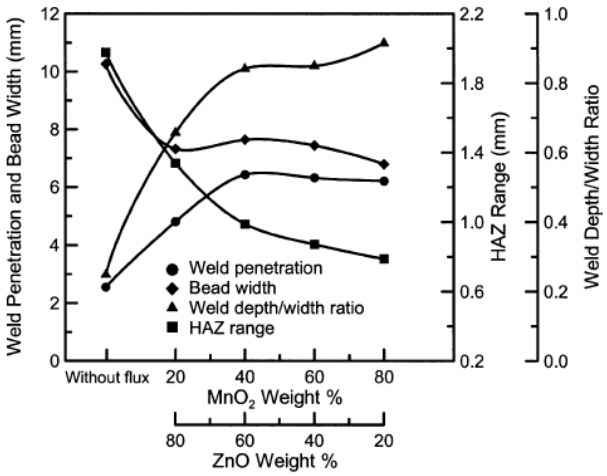

Figure 7: Characteristics of TIG weld geometry produced with various flux composition [22].

The coating thickness is observed to have a very profound effect on weld penetration as shown in Fig. 8 [17]. The maximum of penetration in A-TIG depends on the welding current. Beyond the optimal thickness, weld

penetrations decrease significantly. This rapid fall can be explained by higher energy consumption required to break the flux barrier.

For A-TIG process, a paste is obtained by mixing flux powder in a liquid carrier which is very often alcohol or acetone. A-TIG welding was carried out with the activating fluxes dissolved by acetone, distilled water, ethanol and methyl ethyl ketone (MEK) respectively, the influence of solvent on weld penetration is shown in Fig. 9 [24]. Among the four kinds of solvents, acetone has the most obvious effect, followed by ethanol.

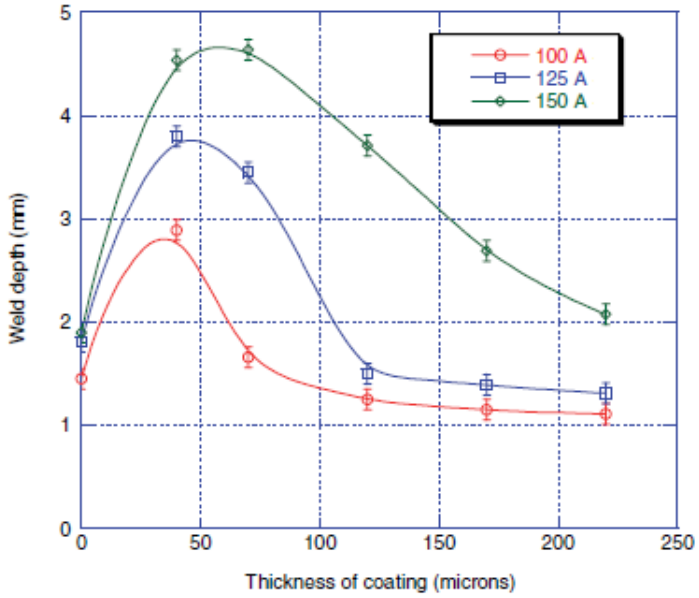

Figure 8: Evolution of penetration depths with coating thickness in A-TIG welding [17].

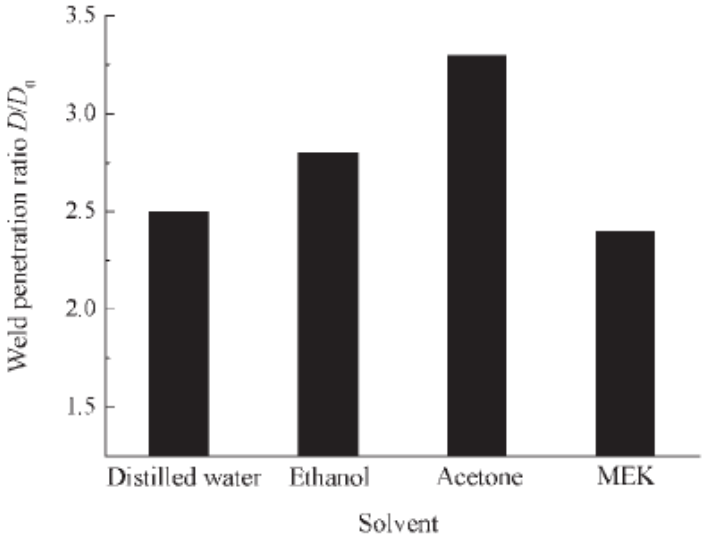

Figure 9: Effect of solvent on weld penetration in A-TIG welding [24].

Effects of A-TIG Welding Parameters

In TIG welding the welding parameters determine the weld bead geometry. The important parameters are the welding current, the arc voltage, the arc length, the welding speed, composition of the shielding gas and the gas flow rate [26]. The effects of these parameters in A-TIG welding are explained below.

The influence of welding current on depth of penetration and weld bead width of the bead-on-plate welds made with and without flux is shown in Fig. 10 respectively, for 304LN steel plates [25]. The increase in welding current causes a higher weld energy and an increase weld cross section area, weld depth and weld width [26]. The growth in weld penetration and width is not equivalent for TIG and A-TIG welding as shown in Fig. 10. It

was found that, at all current levels the increase in depth of penetration in A-TIG welding is almost twice that of conventional TIG welding. It can be seen that the weld bead width of A-TIG welding is enlarged by more than half for the same welding current of TIG welding.

As the welding speed increases, the arc input heat per weld length decreases, and the weld penetration becomes shallow [26]. Fig. 11 shows the measured penetration of autogenous TIG bead-on-plate welds into 5mm thick stainless steel as a function of weld current and travel speed [16]. The penetration depth is inversely proportional to travel speed at a particular weld current. The abilities of oxide fluxes increasing the weld penetration decrease with the increasing of welding speed.

Arc length is critical in determining the arc energy density during TIG welding. Generally, welding with a shorter arc length, the heat of the arc is more readily transferred into the workpiece than diffused to the surrounding environment. To avoid electrode damage and obtain arc stability, austenitic stainless steels A-TIG welding arc length was recommended to be kept in 2-4 mm [25].

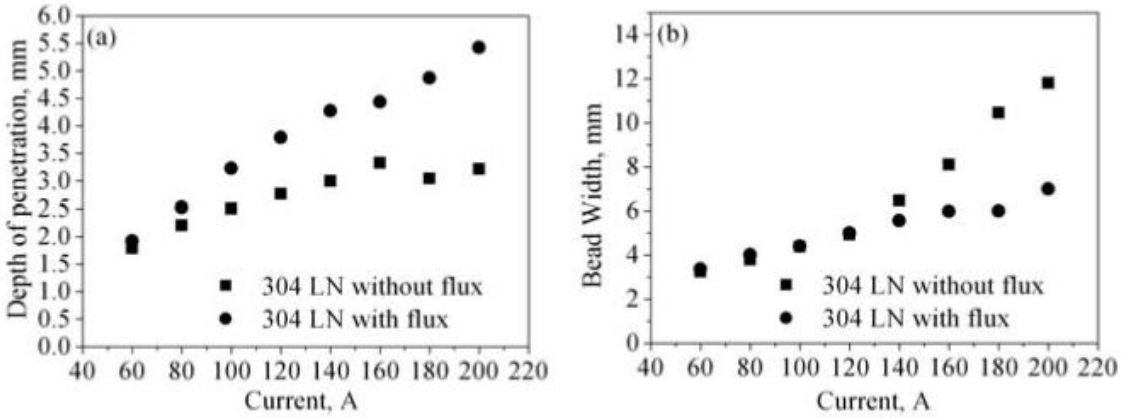

Figure 10: Influence of welding current on the (a) depth of penetration and (b) bead width of the welds produced by TIG and A-TIG welding of 304LN steels [25].

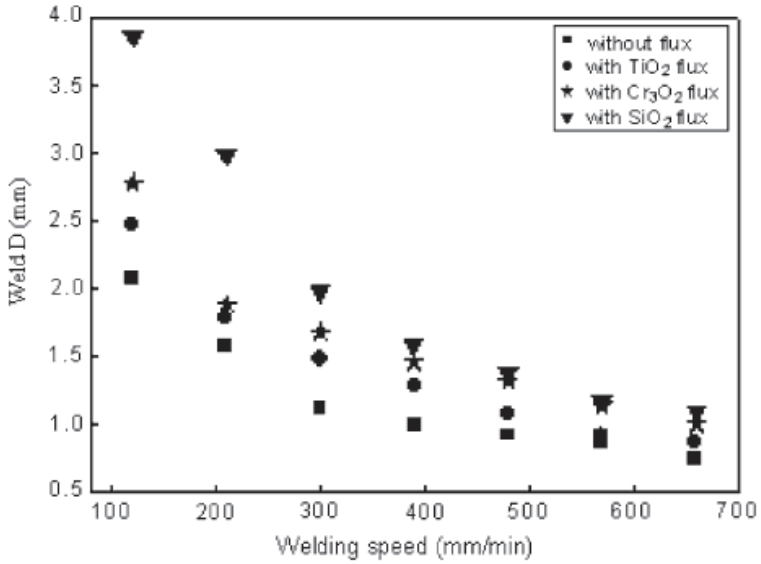

Figure 11: Effect of process parameters on penetration depth of stainless steel TIG welds [16].

In A-TIG welding the arc voltage increases slightly [26]. Fig. 12 shows the effect of TIG welding on arc voltage with and without flux. The weld current and travel speed were maintained at a constant value, and the arc voltage increased when the activated TIG welding was used [20]. The decomposed flux additives attract electrons, causing the arc to constrict and result in an increase in arc voltage [20]. Fig. 14 clearly shows that the five fluxes can simultaneously increase the arc voltage, whereas the increase caused by the oxides can be weak

or strong depending on the flux compositions. There is a clear correlation between the measured arc voltage and the observed arc constriction in TIG welding with and without flux, i.e., the higher the arc voltage value, the greater weld arc constriction will be [20].

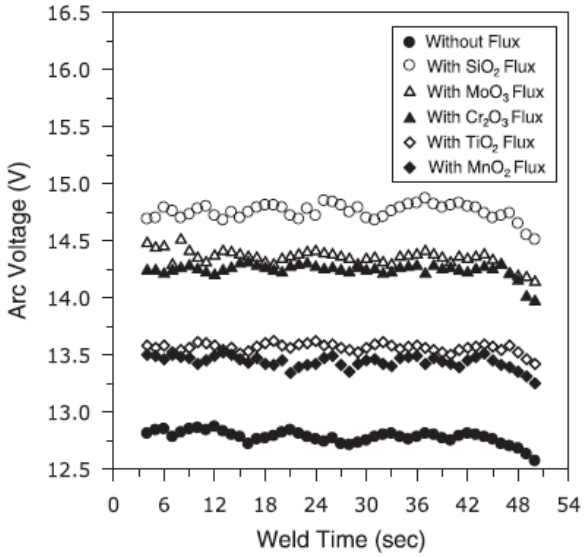

Figure 12: Effect of oxide flux on arc voltage [20].

Argon is the most commonly used for TIG process because it has a relatively low spatter and a stable arc [27]. Helium is another important inert gas for TIG welding. Compared to argon, its current density at the anode spot on the liquid pool under He shielding is high, which will directly increase the electromagnetic force and possibly increase the temperature gradient on the pool surface. Since the strength of the Marangoni convection is controlled by the combination of the temperature gradient on the pool surface and the temperature coefficient of the surface tension, the helium should have a more significant effect on the Marangoni convection [28].

Adding an active element to the weld pool through the shielding gas is another recommended method for deep penetration in TIG welding [27]. A suitable amount of O_2 or CO_2 addition in the shielding gas produced a significant improvement in weld penetration depth [29]. The oxygen in the weld metal from the decomposition of the mixed shielding gas plays an important role in changing the Marangoni convection in the weld pool. When the oxygen concentration in the weld metal is over 70 wt. ppm, the Marangoni convection in the weld pool changes from outward to inward [29]. Consequently, a deep and narrow weld shape forms.

Hydrogen is added to argon for TIG welding of stainless steels [30]. The addition of hydrogen also significantly increases the volume of molten material in the weld pool due to the higher thermal conductivity of argon–hydrogen mixtures at temperatures at which molecules of hydrogen dissociate [31]. In TIG welding the arc voltage also increased with the hydrogen and nitrogen content [32]. Increasing the hydrogen or nitrogen content of the shielding gas contributed to an increase in penetration depth and in the cross-sectional area of the weld metal [32].

Conclusion

The TIG welding process is very sensitive to small changes in the electric arc environment. During A-TIG welding of steels with proper oxide type fluxes, the oxides decompose and the oxygen atoms transfer to the liquid weld pool. If sufficient amount of oxygen is transferred to the weld pool the direction of the Marangoni convection and a deep weld bead geometry forms. Some halides presenting in the flux and the metal atoms coming from the decomposed oxide powders cause arc constriction which is also a useful mechanism to increase the weld depth. The deep penetration depth obtained in A-TIG applications is the main advantage of this process. Deep welds give distinguished savings in welding time and weld costs. Some other advantages of the A-TIG welding process are less welding distortions and higher weld strengths. During A-TIG welding of stainless steels some alloying elements, particularly chrome, may be lost by the increased oxidation in the weld pool.

References

[1]. Ahmed, N. (2005). New developments in advanced welding. Woodhead Publishing Limited, Abington.

[2]. Lucas, W., (2000). Activating flux improving the performance of the TIG process. *Welding and Metal Fabrication*, 2 (12): 7-10.

[3]. Tseng, K.H., Chen, K.L. (2012). Comparisons between TiO_2 and SiO_2 flux assisted TIG welding processes. *Journal of Nanoscience and Nanotechnology*, 12: 6359-6367.

[4]. Sandor, T., Mekler, C., Dobranszky, J., Kaptay, G. (2013). An improved theoretical model for A-TIG welding based on surface phase transition and reversed marangoni flow. *Metallurgical and Materials Transactions A*, 44A: 351-361.

[5]. Tanaka, M. (2005). Effects of surface active elements on weld pool formation using TIG arcs. *Welding International*, 19: 870-876.

[6]. Howse, D.S., Lucas, W. (2000). Investigation into arc constriction by active fluxes for tungsten inert gas welding. *Science and Technology of Welding and Joining*, 5: 189-193.

[7]. Tseng, K.H. (2013). Development and application of oxide-based flux powder for tungsten inert gas welding of austenitic stainless steels, *Powder Technology*, 233: 72-79.

[8]. Simonik, A.G. (1976). The effect of contraction of the arc discharge upon the introduction of electro-negative elements. *Welding Production*, 3: 49-51.

[9]. Yukler, A.I. (1992). Weld metal. *MUTEF Publications*, Istanbul, 1992.

[10]. Lowke, J. J., Tanaka, M., Ushio, M. (2005). Mechanisms giving increased weld depth due to a flux, *Journal of Physics D: Applied Physics*, 38: 3438-3445.

[11]. Zhang, R.H., Pan, J.I., Katayama, S. (2011). The mechanism of penetration increase in A-TIG welding. *Frontiers of Materials Science*, 5: 109-118.

[12]. Berthier, A., Paillard, P.,Carin, M., Valensi, F., Pellerin, S. (2012). TIG and A-TIG welding experimental investigations and comparison to simulation Part 1: Identification of Marangoni effect. *Science and Technology of Welding and Joining*, 17: 609-615.

[13]. US Patent No.8097826 B2. (2012). Penetration enhancing flux formulation for tungsten inert gas (TIG) welding of austenitic stainless steel and its application.

[14]. Hu, S.,Wang, Y.,Shen, J.,Chen, C.H. (2013). A-TIG welding of 430 ferritic stainless steel. *Journal of Tianjin University (Science and Technology)*, 46: 831-835.

[15]. Huang, H.Y., Shyu, S.W., Tseng, K H., Chou, C.P. (2006). Effects of the process parameters on austenitic stainless steel by TIG-flux welding. *Journal of Materials Science and Technology*, 22: 367-374.

[16]. Tseng, K.H., Chuang, K.J. (2012). Application of iron-based powders in tungsten inert gas welding for 17Cr–10Ni–2Mo alloys. *Powder Technology*, 228: 36-46.

[17]. Ruckert, G. (2005). Etude de la contribution des flux activants en soudage A-TIG. *These de Doctorat, Ecole Centrale de Nantes et l' Universite de*, Nantes.

[18]. Dhandha, K.H., Badheka, V.J. (2015). Effect of activating fluxes on weld bead morphology of P91 steel bead-on-plate welds by flux assisted tungsten inert gas welding process. *Journal of Manufacturing Processes*,17: 48-57.

[19]. Modenesi, P.J., Apolinario, E.R., Pereira, I.M. (2000). TIG welding with single-component fluxes. *Journal of Materials Processing Technology*, 99: 260-265.

[20]. Chern, T.S., Tseng, K.H., Tsai, H.L. (2011). Study of the characteristics of duplex stainless steel activated tungsten inert gas welds. *Materials and Design*, 32: 255-263.

[21]. Vora, J., Badheka, V. (2015). Experimental investigation on mechanism and weld morphology of activated TIG welded bead-on-plate weldments of reduced activation ferritic/martensitic steel using oxide fluxes. *Journal of Manufacturing Processes*, 20: 224-233.

[22]. Huang, H.Y., Shyu, S.W., Tseng, K.H., Chou, C.P. (2005). Evaluation of TIG flux welding on the characteristics of stainless steel", *Science and Technology of Welding and Joining*,10: 566-573.

[23]. Lu, S., Fujii, H., Sugiyama, H., Nogi, K. (2003). Mechanism and optimization of oxide fluxes for deep penetration in gas tungsten arc welding. *Metallurgical and Materials Transactions A*, 34A: 1901-1907.
[24]. Huang, H., Fan, Y., Shao, D.F. (2012). Alternative current flux zoned tungsten inert gas welding process for aluminum alloys. *Science and Technology of Welding and Joining*, 17: 122-127.
[25]. Surinder, T., Anirban, B. (2016). Activated-TIG welding of different steels: influence of various flux and shielding gas. *Materials and Manufacturing Processes*, 31: 335–342.
[26]. Li, Q.M., Wang, X.H., Zou, Z., Wu, D.J. (2007). Effect of activating flux on arc shape and arc voltage in tungsten inert gas welding. *Transactions of Nonferrous Metals Society of China*, 17:486-490.
[27]. Lucas, W. (1990). TIG and plasma welding, Woodhead Publishing Ltd, Cambridge.
[28]. Loureiro, A.R., Costa, B.F.O., Batista, A.C., Rodrigues, A. (2009). Effect of activating flux and shielding gas on microstructure of TIG welds in austenitic stainless steel. *Science and Technology of Welding and Joining*, 14: 615-620.
[29]. Lu, S., Fujii, H., Nogi, K. (2009). Arc ignitability, bead protection and weld shape variations for He-Ar-O_2 shielded GTA welding on SUS304 stainless steel. *Journal of Materials Processing Technology*, 209: 1231-1239.
[30]. Durgutlu, A. (2004). Experimental investigation of the effect of hydrogen in argon as a shielding gas on TIG welding of austenitic stainless steel. *Materials and Design*, 25: 19-23.
[31]. Lowke, J.J. Richard, M.H., Jawad, Anthony, M.B. (1997). Prediction of gas tungsten arc welding properties in mixtures of argon and hydrogen. *IEEE Transactions of Plasma Science*, 25: 925-930.
[32]. Huang, H.Y. (2009). Effects of shielding gas composition and activating flux on GTAW weldments. *Materials and Design*, 30: 2404-2409.